Biochemistry

pubs.acs.org/biochemistry Article

Structural Analysis of the Effect of a Dual-FLAG Tag on Transthyretin

Mehdi Shirzadeh, Michael L. Poltash, Arthur Laganowsky, and David H. Russell*

Cite This: *Biochemistry* 2020, 59, 1013–1022 Read Online

ACCESS | Metrics & More | Article Recommendations | Supporting Information

ABSTRACT: Recombinant proteins have increased our knowledge regarding the physiological role of proteins; however, affinity purification tags are often not cleaved prior to analysis, and their effects on protein structure, stability and assembly are often overlooked. In this study, the stabilizing effects of an N-terminus dual-FLAG (FT_2) tag fusion to transthyretin (TTR), a construct used in previous studies, are investigated using native ion mobility-mass spectrometry (IM-MS). A combination of collision-induced unfolding and variable-temperature electrospray ionization is used to compare gas- and solution-phase stabilities of FT_2-TTR to wild-type and C-terminal tagged TTR. Despite an increased stability of both gas- and solution-phase FT_2-TTR, thermal degradation of FT_2-TTR was observed at elevated temperatures, viz., backbone cleavage occurring between Lys9 and Cys10. This cleavage reaction is consistent with previously reported metalloprotease activity of TTR [Liz et al. 2009] and is suppressed by either metal chelation or excess zinc. This study brings to the fore the effect of affinity tag stabilization of TTR and emphasizes unprecedented detail afforded by native IM-MS to assess structural discrepancies of recombinant proteins from their wild-type counterparts.

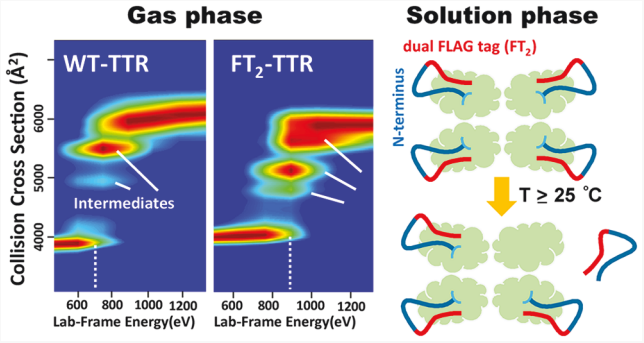

The biophysics of transthyretin (TTR), a homotetrameric protein complex with a β-sandwich fold,[1] involved in thyroxine (T_4) transport in cerebrospinal fluid (CSF) and retinol in blood,[2−5] has been the subject of many studies.[6−9] Although many studies have linked TTR to amyloid diseases, understanding the genetic and pathological maladies remains elusive. While it is generally agreed that TTR plays a key role in disease progression, how TTR structure and stability influence the mechanism(s) by which aggregates are formed remains poorly understood.[10] Development of a biological mechanism for aggregation is difficult because it is still unclear as to which particular species, viz., transient intermediates (kinetic and/or thermodynamic), are involved; possibly of greater importance are the structure(s) and stabilities of these toxic species. X-ray crystallography and nuclear magnetic resonance (NMR), in concert with more traditional biophysical techniques, have provided atomistic level structure(s) for TTR. Unfortunately, traditional biophysical techniques are not well suited for studies of heterogeneous systems, especially those where low abundance transient intermediates are responsible for disease. For example, TTR functions as a metallopeptidase[11] when complexed with Zn(II), for which three distinct sites have been determined.[12] Excess Zn(II) binding decreases retinol transport function[12] and increases rates of fibril formation for the TTR L55P mutant.[13] Moreover, changes in structure/stability occur upon binding Zn^{2+}, which might ultimately influence T_4 or retinol binding. The new evidence for metal-induced oxidation observed using native IM-MS underscores the importance of rigorous analytical measurements to understand protein behavior.[14]

An equally important aspect of understanding protein function and structure lies in the advances made in the expression and purification of recombinant proteins. Overexpressed proteins are typically expressed and isolated using a specific affinity tag, such as polyhistidine (6 × His), FLAG (DYKDDDDK), and Strep tag.[15,16] Despite their applicability and advantages, the impact of tags on structure, stability, and function of proteins is often overlooked.[17] For instance, an increase in backbone dynamics of tagged proteins has been reported[17] based on an increase in B-factor of their crystal structures, which can promote in-body aggregation or decreased solubility. Booth et al. have reported slightly enhanced thermal stability of proteins without the N-terminal polyhistidine tag compared to tagged proteins.[18] Yewdall and co-workers have also shown that tags can have aberrant effects on oligomerization of toroidal proteins and disfavor their self-assembly.[19] Chemical modification of tags has been also reported for the well-studied polyhistidine tag in which α-*N*-6-phosphogluconoylation of the tag results in an increase in mass

Received: February 5, 2020
Revised: February 25, 2020
Published: February 26, 2020

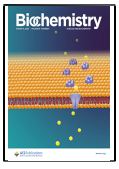

https://dx.doi.org/10.1021/acs.biochem.0c00105
Biochemistry 2020, 59, 1013−1022

Table 1. Summary of Fusion Tags for WT-TTR, CT-TTR, and FT_2-TTR[a]

	sequence	MW (monomer, Da)	pI
WT-TTR	**GS**GPTGTGESKCPLM...PKE	13905	5.31
CT-TTR	MGPTGTGESKCPLM...PKE***ASGENLFYQ***	14903	5.15
FT_2-TTR	**GS***DYKDDDDKDYKDDDDK*GPTG...PKE	15895	4.69

[a]The amino acid sequence shown in bold is the remainder after TEV protease cleavage. For CT-TTR, bold amino acids were used to increase the TTR molecular weight for the subunit exchange experiments.[42] The italic amino acid sequence corresponds to the FT_2 tag in the N-terminus of FT_2-TTR.

by 178 and 258 Da.[20] More recently, Liu et al. reported previously unidentified phosphorylation sites of a G-protein-gated inward rectifying potassium channel (GIRK2), and phosphorylation sites were found on both the surface exposed regions of the protein as well as the serine residues of the linker region between GIRK2 and TEV protease cleavage sites.[21]

Tag removal generally increases the purification time as well as sample purity, and several studies have reported beneficial or no effect of retaining the tag on proteins.[17,22−25] The decision to cleave or retain the tag is difficult because molecular level details of the influence of the tags are lacking. Although structural effects of tags can be obtained using high-resolution biophysical methods such as X-ray crystallography and NMR, the requirements for crystallization and limitation on size makes these methods less appealing. Differential scanning calorimetry (DSC)[26] and circular dichroism (CD) spectroscopy,[27] which are experimentally less complicated, can be used to compare protein stabilities, but these methods do not offer molecular-level details. Fluorescence-based assays, i.e., differential scanning fluorimetry (DSF) or thermal shift assay (TSA),[28,29] can indirectly measure protein stability through monitoring unfolding and subsequent binding of a fluorescent dye to the exposed hydrophobic residues, but the dyes used in this approach can also interact with the protein and thereby alter its stability.

Native ion mobility-mass spectrometry (IM-MS),[30,31] on the other hand, has emerged as a fast and powerful technique for structural biology and offers information regarding stoichiometry,[32,33] protein−protein interactions,[34] and the thermodynamics and kinetics of ligand binding to proteins and other biomolecules.[35] The measurement of shape and conformation afforded by ion mobility bodes well for native IM-MS as a potential method to screen and assess protein stability. Specifically, collision-induced unfolding (CIU) offers invaluable information regarding solvent-free unfolding pathways and stability in the gas phase.[36−38]

Recombinant TTR has been extensively used to investigate the underlying mechanism of fibril formation or subunit exchange studies; however, purification tags are often not cleaved.[39−41] Such modifications can alter structure and stability of TTR but such effects have not been extensively investigated. In an earlier study on the subunit exchange of wild-type TTR (WT),[42] the effects of two different tags, dual-FLAG (FT_2) and C-terminal (CT), were examined. FT_2-TTR has a lower isoelectric point (pI) (see Table 1), which facilitates the separation of subunit exchange products using ion exchange chromatography. Rappley et al. have previously reported results from chromatography studies, where a peak that eluted before tetrameric FT_2-TTR corresponded to an impurity, which was believed to come from the loss of one FT_2 tag.[43] Interestingly, we have also noted a backbone cleavage of FT_2-TTR, viz., Lys9-Cys10 (≥24 °C), which complicates subunit exchange experiments and hinders kinetics modeling.[42]

Here, we report native IM-MS studies aimed at characterizing the impact of these fusion tags on TTR and the mechanism of the underlying cleavage for FT_2-TTR. This study utilizes CIU measurements to analyze the gas-phase stability of TTR, and the solution-phase stabilities are studied using a variable-temperature electrospray ionization (VT-ESI) source and collision-induced dissociation (CID). Overall, our results reveal detailed information on the impact of an affinity tag, FT_2, on TTR structure and the mechanism of thermo-cleavage.

EXPERIMENTAL SECTION

Materials. Alcohol dehydrogenase (ADH), concavalin A (ConA), pyruvate kinase (PK), sodium iodide, zinc acetate, copper acetate, tartaric acid, *N*-ethylmaleimide (NEM), tris (2-carboxyethyl)phosphine hydrochloride (TCEP), triethylammonium acetate (TEAA), diethylenetriaminepentaacetic acid (DTPA), and formic acid (FA) were purchased from Sigma-Aldrich (St. Louis, MO). Ammonium acetate (AA) was purchased from EMD (Millipore). Thyroxine (T_4), dimethyl sulfoxide (DMSO), acetonitrile (ACN), methanol (MeOH), and platinum wire (99.9%) were purchased from Alfa Aesar (Ward Hill, MA).

Protein Purification. Methodologies used for the expression of the TTR variants have been described previously.[42] Briefly, plasmids for TTR variants were transformed into *E. coli* cells. Colonies were grown in LB media (IBI Scientific) at 37 °C until an OD_{600} of 0.6−1.0. Isopropyl *β-d*-1-thiogalactopyranoside (IPTG) (Enzo Life Sciences Inc.) was used at a final concentration of 0.5 mM to induce cells. Incubation was performed for 3−4 h at 37 °C. Cells were then harvested and centrifuged to remove cellular debris and loaded on a HisTrap HP column. Bound proteins were eluted with high imidazole buffer (500 mM) and immediately loaded to a desalting column (HiPrep 26/10). The His tag and fused protein (MBP for WT- and FT_2-TTR and GFP for CT-TTR) were cleaved using TEV protease overnight at 4 °C. Size-exclusion chromatography (SEC) was used to separate aggregates and cleaved tags from TTR variants, and purified proteins were flash frozen and stored at −80 °C.

Native Ion Mobility-Mass Spectrometry. A Synapt G2 traveling wave ion mobility separation (TWIMS) instrument (Waters, U.K.) was used for the native IM-MS experiments. A static nano-ESI source and in-house pulled borosilicate capillary tips were used to introduce TTR samples. Important tuning parameters are shown in Table S1. Mass calibration was performed using NaI, 2 mg/mL in ACN/H_2O/FA (49:49:1) for 250−3000 *m*/*z*. This calibration is sufficient to accurately assign and perform top down analysis for thermo-cleaved peptides (see Supporting Information). Cesium iodide, 2 mg/mL in ACN/MeOH/H_2O (30:30:40), was used as the calibrant for intact protein analysis (250−4500 *m*/*z*). The

https://dx.doi.org/10.1021/acs.biochem.0c00105
Biochemistry 2020, 59, 1013−1022

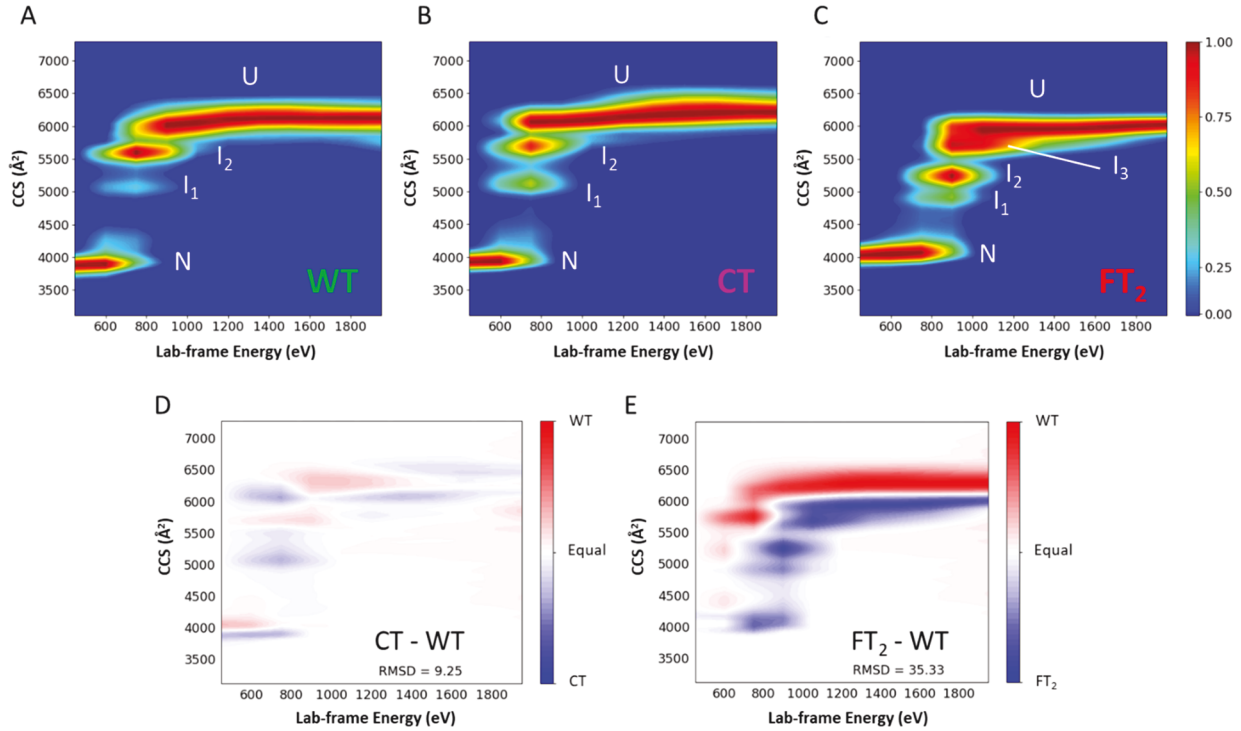

Figure 1. Different gas-phase stabilities and intermediates were observed for TTRs (untagged and tagged) in the gas phase. Lab-frame energy is plotted versus the collision cross section (CCS) of (A) WT-TTR (B) CT-TTR, and (C) FT_2-TTR (15+) in 200 mM ammonium acetate at 25 °C. Difference CIU plot obtained from te subtraction of (D) CT-TTR and WT-TTR and (E) FT_2-TTR and WT-TTR after adjustment of the CCS value of the native conformer of WT-TTR to match the CCS value of the native conformer of CT-TTR or FT_2-TTR. CIU plots of WT- and CT-TTR are similar in terms of the number of intermediates and the relative energy required for unfolding at each step (see text for more detail), whereas FT_2-TTR shows a third intermediate and different unfolding energies.

MS spectra for intact proteins were minimally smoothed without background subtraction.

Theoretical masses and isoelectric points (pI) of the proteins were calculated using the ExPASy server. Proteins (final concentration of 5 μM) were buffer exchanged into 200 mM AA (pH = 6.8) using Biospin columns, 6 kDa cutoff (BioRad). TEAA (100 mM) was used to generate charge reduced mass spectra of TTR. Stock solutions of T_4 (12 mM) were prepared in DMSO and further diluted with 200 mM AA (final DMSO concentration <5%). For CIU experiments, mass selected ions were activated via collision with buffer gas (argon) to increase the internal energy of ions, which subsequently results in gas-phase unfolding. CIUSuite 2[44] was used to generate CIU heat maps of the collision cross section (CCS) versus lab-frame energy (E_{lab} = collision voltage × charge). CCS calculations were performed as described elsewhere.[45] ADH, ConA, and PK were used as calibrants, and corresponding CCS values were obtained from literature.[46]

Circular Dichroism Spectroscopy. CD spectra were collected using a Chirascan CD spectrometer from Applied Photophysics, Ltd. with a 10 mm path length quartz cell for a protein concentration of 3.6 μM in 10 mM Na_2HPO_4, pH 7.4. Data are averaged from two replicates collected with a 0.5 nm bandwidth ranging from 200 to 250 nm at room temperature. CD melting experiments were performed using a Peltier sample holder to heat the sample from 30 to 90 °C at 3 °C/min at 220 nm.

Variable-Temperature Electrospray Ionization Apparatus. VT-ESI experiments were performed using a home-built ESI heater, adapted from a similar design previously employed via Sterling et al.[47] (Figure S1). The heater consists of a capillary holder that is designed to also hold a thermally conductive, electrically insulating ceramic housing that surrounds the ESI needle. A kanthal wire is coiled around the ceramic cylinder, and the resistively heated kanthal wire transfers heat to the ceramic housing and the solution contained in the ESI needle. This device can heat from just above ambient to more than 100 °C. Solution temperatures were calibrated by inserting a microthermocouple into the ESI needle that contained only AA. Fresh TTR samples were loaded for each temperature measurement (n = 3) to avoid metal-induced oxidation during ESI.[14]

Quantification of Thermo-Cleaved Peptide of FT_2-TTR. To assess the effect of solution conditions on FT_2-TTR cleavage upon heating, protein aliquots (9 uL, 13 μM) in 200 mM ammonium acetate were mixed with 1 μL of zinc acetate (100 μM, 1000 μM, and 28 mM), copper acetate (100 μM), DTPA (10 mM), and TCEP (10 mM). Mixtures were incubated for 3 days at 50 °C and subsequently separated using Ziptip (C18 column, Thermo Fisher) and eluted with a 20 μL solution containing 30% ACN and 0.1% FA. The measured signal for samples (n = 3) collected with three different tips was converted to a relative amount of the thermo-cleaved peptide.

Separation of the Thermo-Cleaved Peptide from FT_2-TTR. Both size-exclusion chromatography (16/600 75 pg column eluted with 20 mM Tris, 50 mM NaCl, pH = 7.4) and hydrophobic interaction chromatography (HiTrap Phenyl HP, 5 mL column (GE Healthcare) eluted with 20 mM Tris, 500 mM NaCl, pH = 8.0) were used to separate the thermo-cleaved peptide from thermally heated FT_2-TTR. Due to the strong interaction between the thermo-cleaved peptide and

https://dx.doi.org/10.1021/acs.biochem.0c00105
Biochemistry 2020, 59, 1013−1022

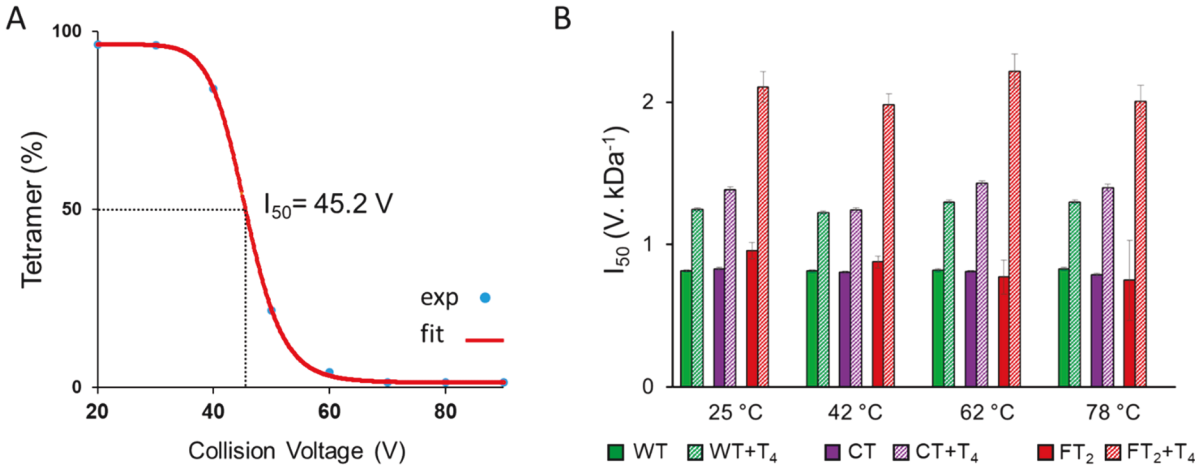

Figure 2. Solution-phase stability analysis of TTR variants using a VT-ESI source. (A) Relative abundance of tetrameric WT-TTR to total ions as a function of collision voltage (25 °C). Data are fitted with an exponential fit to get I_{50}, which represents the voltage that 50% of tetramers remains intact. (B) I_{50} values for WT-, CT-, and FT_2-TTR at 25, 42, 62, and 78 °C without (solid) and with (dashed) T_4 in a 1:2 molar ratio (TTR/T_4). Measurements are obtained for three different replicates (n = 3) with error bars shown as ± standard deviation.

truncated TTR, both experiments failed to separate them. Denaturing conditions using ZipTip with elution solution consisting of 10% acetonitrile and 0.1% FA were used to elute only the peptide (the usage of more hydrophobic solvent (ACN > 10%) led to elution of peptide and unfolded monomers). The solvent was evaporated using a Savant Speed Vac (Thermo Savant, Holbrook, NY), and 200 mM ammonium acetate was used to dissolve the peptide.

Zinc and Copper Binding Affinity to the Thermo-Cleaved Peptide. Purified thermo-cleaved peptide samples were incubated with 2 μM and 20 μM zinc acetate and copper acetate. The mass spectrum of the sample incubated with 20 μM copper showed complete binding to the peptide, whereas, for samples incubated with 2 μM and 20 μM zinc acetate, a similar relative abundance of the holo peak was observed. To avoid nonspecific binding during nanoelectrospray ionization, similar experiments were performed in the presence of 1 mM tartaric acid as a competitive binding specie to metals,[48] and no significant differences were observed with or without it.

RESULTS

FT_2 Tag Increases TTR Resistant to Unfold in the Gas Phase. CIU is a process by which ions are activated by energetic collisions with a neutral target gas, such as Ar, and changes in the CCS of the ions are monitored by using IM-MS.[49] This approach is increasingly used to investigate the effects of ligands,[37,50] small molecule,[51,52] and/or metal binding[53] on the structure and stabilities of the gas-phase ions. Here, CIU is used to compare the stabilities and structures of WT-, CT-, and FT_2-TTR. Figure 1 contains CIU heat maps for the 15^+ ions of WT-, CT-, and FT_2-TTR sprayed from ammonium acetate. Unfolding transitions of the native conformer (N) produce several intermediates, labeled I_1, I_2 (and I_3 in case of FT_2-TTR), and the unfolded conformer (U). Interestingly, the CIU heat maps for CT- and WT-TTR are quite similar; however, FT_2-TTR appears to stabilize TTR against unfolding, as evidenced by the shift in the collision energy required to form the first intermediate (I_1), i.e., E_{lab} ~ 870 eV for FT_2-TTR vs ~700 eV and ~730 eV for WT and CT-TTR, respectively. Also, the CIU heat maps CT−WT and FT_2−WT clearly show that the unfolding pathway of WT-TTR is similar to CT-TTR but very different from FT_2-TTR (Figure 1D,E). The enhanced stability of FT_2-TTR is even more pronounced for charge-reduced TTRs 11^+ ions as FT_2-TTR retains its native conformer even at the highest activation energy (1900 eV), whereas WT-TTR unfolds to I_1 at ~800 eV (see Figure S2). The increased stability of FT_2-TTR, compared to two other proteins (Figure S3), independent of their charge and mass, was confirmed (see Supporting Information). Note that we did not include data for ions that have even charges as these signals overlap with signals for dimer ions (Figure S4).

The observation of a third intermediate (I_3) in the CIU for FT_2-TTR suggests that the FT_2 tag alters the protein unfolding pathway. Ruotolo et al. previously reported the correlation between the number of domains and the observed CIU intermediates.[54,55] The difference heat maps (Figure 1D,E) suggest that intermediates from WT and CT most likely are produced from the unfolding of similar domains of TTR. The calculated relative ratios of CCS values for unfolding products, CT- and FT_2-TTR, compared to WT-TTR (see Table S2 and Figure S5 for more detail), show that I_1 in FT_2 appears at lower CCS, compared to WT- and CT-TTR, suggesting that it might originate from the unfolding of a new domain, resulting from the FT_2 tag infusion in the protein. CD spectra of three proteins (Figure S6A) showed no significant changes in the secondary structure of TTR variants, which cannot provide any insight into observed discrepancies in CIU experiments.

Temperature Effect on the Quaternary Structure of FT_2-TTR. VT-ESI, in combination with native IM-MS, can provide similar information as calorimetric methods,[56−58] specifically on thermodynamics and melting point temperatures of protein and protein complexes.[35] This apparatus (Figure S1) is used to measure the effects of temperature on the quaternary structure of TTR and to compare the thermal stability of TTR with various tags. An increase in the average charge state (z_{avg}) of monomeric proteins has been correlated to protein unfolding;[56,59] however, only subtle shifts in the z_{avg} of TTR upon heating are observed in this study. This observation reflects the high thermostability of TTR (T_m > 98 °C);[60] however, previous studies have shown that the tetramer−dimer and dimer−monomer equilibrium is highly temperature-dependent.[42] For example, higher dissociation rates are observed for dimer to monomer reactions as the

https://dx.doi.org/10.1021/acs.biochem.0c00105
Biochemistry 2020, 59, 1013−1022

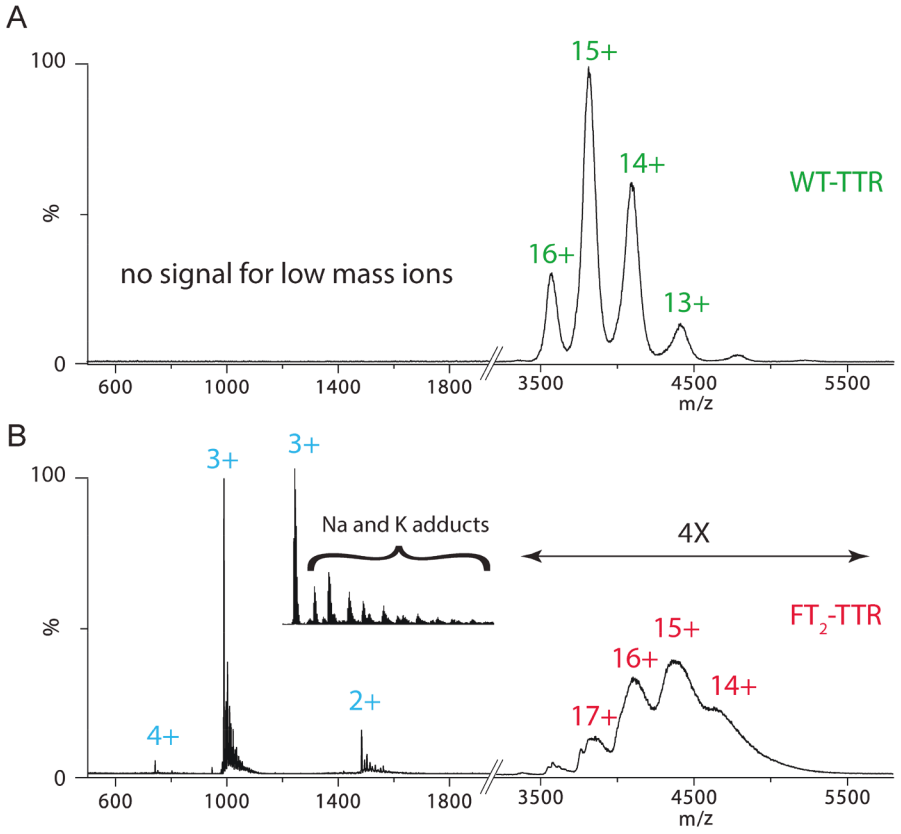

Figure 3. Thermo-cleavage of FT_2-TTR at above ambient temperature. Mass spectra of (A) WT-TTR and (B) FT_2-TTR incubated at 50 °C for 18 h. Only FT_2-TTR upon heating produces a thermo-cleaved peptide, which is extensively bound to Na and K ions (charge states are shown in blue).

solution temperature is increased,[42] and higher temperatures decrease the rate of tetramer to dimer reactions. Collision-induced dissociation (CID) of TTR results in monomer ejection in the gas phase, which requires interrupting interactions in both the dimer−dimer and monomer−monomer interfaces. Upon transition to the gas phase, ions can retain their solution-phase structure;[61,62] thus, CID of TTR variants originating from solutions that have different temperatures can be used to track changes in the quaternary structure upon heating. This approach provides yet another means to compare stabilities of protein complexes, viz., untagged vs tagged TTRs.

Here, in VT-ESI experiments, the relative abundances of tetrameric ions versus collision voltage are used to measure the point, denoted as I_{50}, at which 50% of the tetramer remains intact (Figure 2A). Higher I_{50} values indicate more energy is required for gas-phase dissociation of the protein. Similar to unfolding energies, the I_{50} values are normalized for differences in mass due to tag infusion (Figure 2B). For WT- and CT-TTR, similar normalized I_{50} values were obtained over a wide range of temperatures (25−78 °C), indicative of their similar and high thermal stabilities (Figure 2B). An increased stability for FT_2-TTR, relative to WT-TTR (I_{50} of 0.95 ± 0.05 vs 0.81 ± 0.007 V/kDa), is consistent with CIU results, and similar results were obtained for charge reduced ions (Figure S7A). These results indicate higher relative gas- and solution-phase stabilities for FT_2-TTR, compared to WT- and CT-TTR. While no significant change in I_{50} was observed for WT- and CT-TTR over a range of temperatures (25−78 °C), the stability of FT_2-TTR gradually decreases with increasing temperatures. Measurements shown in Figure 2 were performed in three replicates (n = 3) for each temperature (25, 42, 62, and 78 °C), and data reproducibility is diminished for FT_2-TTR at elevated temperatures (Table S3). The thermal stability of TTR samples was also investigated by using CD spectroscopy to monitor secondary structure changes (Figure S6B). In these experiments, no melting was observed for three variants in the temperature range of 30−90 °C; however, there was a similar reproducibility issue and slightly lower stability of FT_2-TTR (Figure S8).

VT-ESI was also used to examine the effects of the TTR-T_4 complex; T_4 is known to stabilize the TTR quaternary structure. At 25 °C (Figure 2B), the I_{50} values for apo/holo proteins are 0.82:1.3, 0.82:1.4, and 0.88:2.1 V/kDa for WT-, CT-, and FT_2-TTR, respectively. Note the ∼2-fold increase for FT_2-TTR, compared to WT-TTR and CT-TTR, upon T_4 binding. Enhanced stabilities were also obtained for the TTR-T_4 complex, compared to apo proteins at higher temperatures (Figure 2B). Such differences can be due to a higher affinity of FT_2-TTR to T_4; however, our results showed a relatively similar binding affinity for WT and FT_2-TTR and a slightly higher affinity for CT-TTR. Thus, these data suggest that the increased temperature destabilizes the FT_2-TTR quaternary structure, whereas it has no effect on WT-TTR or CT-TTR.

Backbone Cleavage Observed only for FT_2-TTR upon Heating. The temperature-dependent degradation of FT_2-TTR was reported in a previous paper, describing subunit exchange experiments.[42] To better understand the underlying mechanism(s) and to identify the cleavage site, mass spectra of both WT- and FT_2-TTR were acquired for samples incubated at 50 °C for 18 h. Relatively broad peaks were observed for heated WT-TTR solution (3300−4500 m/z) compared to

https://dx.doi.org/10.1021/acs.biochem.0c00105
Biochemistry 2020, 59, 1013−1022

freshly prepared samples (Figure 3A). The observed peak broadening is due to adduction of unidentified salts to the intact molecule,[58] which are removed upon mild gas-phase collisional activation (data not shown). The native MS spectrum of heated FT_2-TTR solution contains abundant signals for multiply charged ions (2+ (1483.632 m/z), 3+ (989.420 m/z), and 4+ (594.051 m/z)), corresponding to an ion with MW = 2965.264 (theoretical: 2965.229) (Figure 3B). In-source activation resulted in the removal of adducts from ions in high m/z (3000−5500) and resolved ions, corresponding to the tetrameric FT_2-TTR with zero, one, and two truncated subunits, as well as the released intact and truncated monomers (Figure S9).

Top down tandem mass spectrometry was used to identify the 2965.264 ion as GSDYKDDDDKDYKDDDDKGPTGTGESK[9] that is formed by the cleavage of Lys9-Cys10 in FT_2-TTR, hereafter denoted as the "thermo-cleaved" peptide (Table S4). Further evidence in support of this assignment is the number of Na^+ and K^+ adduct ions bound to the thermo-cleaved peptide (up to 11 sodium). The formation of salt adducts is consistent with previous studies,[63,64] in which the number of salt adduction is correlated to the number of acidic residues (eight aspartic acids in FT_2 tag). Two other degradation products were also observed with MW = 2750.12 (theoretical: 2750.10) and 2837.15 Da (theoretical: 2837.13) formed by the cleavage of Glu7 and Ser8 with a relative abundance of ∼12% and 4%, respectively. Due to their low abundance, the following discussion is limited to the major thermo-cleaved peptide (Lys9-Cys10 cleavage).

Why Does FT_2 Increase TTR Stability in Gas and Solution Phases? Results from CIU and CID experiments demonstrate increased stability of FT_2-TTR compared to WT- and CT-TTR at room temperature. This enhanced stability is most likely due to the FT_2 interaction with the TTR backbone, but it is unclear as to which amino acid residues are involved in the interactions. To answer this question, a solution containing WT-TTR and the thermo-cleaved peptide was incubated at 24 °C for 18 h (200 mM AA). Interestingly, binding of the thermo-cleaved peptide was not detected, which points to a potential intramolecular interaction of the FT_2 tag (DYKDDDDKDYKDDDDK) with the N-terminal residues of TTR (GPTGTGESK) in the peptide. Nevertheless, we cannot rule out the possibility of structural discrepancies between the intact and isolated tag due to the rigorous isolation process (see Experimental Section). The organic solvent and low pH required to separate the thermo-cleaved peptide may have induced an irreversible change on the structure of the tag, which can prevent its interaction with similar residues on WT-TTR.

Metal-induced oxidation of WT-TTR[14] was also observed in the presence of the thermo-cleaved peptide. Cys-10 oxidation and following Cys10-Pro11 cleavage results in tetrameric WT-TTR with truncated subunits shown in Figure 4 and was also evident in monomers obtained from CID of WT-TTR (data not shown). We further characterized this enhanced oxidation in the presence of the peptide (see Supporting Information), and our results revealed the higher affinity of the peptide to copper (Figure S10), which can potentially (Figure S11) increase the metal-induced oxidation of TTR as previously reported.[14]

Mechanism of Thermo-Cleavage Observed for FT_2-TTR. Thermal degradation of the peptide bond in C-terminus aspartic[65] acid and N-terminus cysteine[66] has been previously

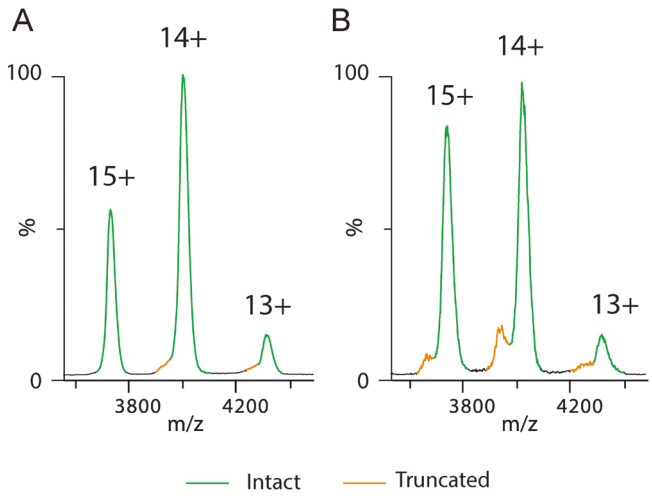

Figure 4. Addition of the thermo-cleaved peptide results in metal-induced oxidation of WT-TTR. Mass spectra of WT-TTR incubated at 24 °C for 72 h. (A) Without and (B) with the thermo-cleaved peptide (GSDYKDDDDKDYKDDDDKGPTGTGESK[9]).

reported for proteins incubated at elevated (220 °C) temperatures. Basile et al. showed that cysteine oxidation is a prerequisite for cysteine degradation and, under a nitrogen atmosphere, is completely diminished.[66] Observed thermo-cleavage (Lys9-Cys10) in our experiment can be the result of thermal decomposition of N-terminus cysteine reported by Basile; however, alkylation of Cys10 with NEM has no significant effect on the amount of thermo-cleaved product. Also, upon addition of TCEP, which inhibits Cys-10 oxidation,[14] the abundance of the thermo-cleaved peptide was increased (Figure 5). These results suggest that cysteine degradation is not responsible for observed thermo-cleavage of FT_2-TTR. Moreover, WT-TTR was not susceptible to thermal decomposition, which raises the question regarding the role of

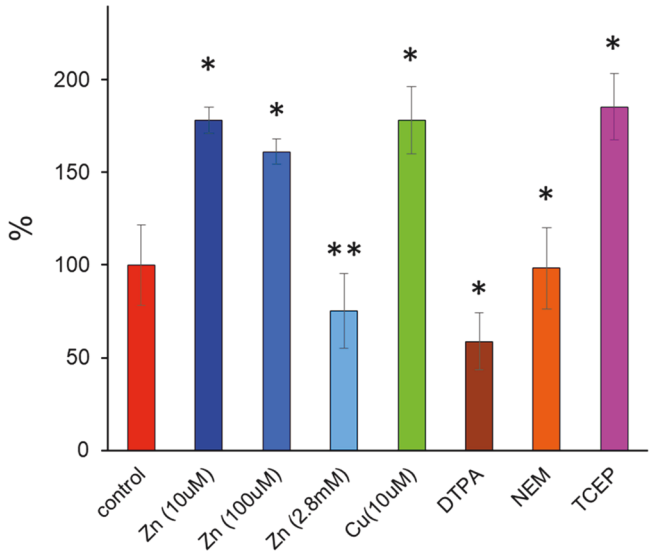

Figure 5. Effect of metal and additives on the amount of FT_2-TTR thermo-cleavage. The relative abundance of the thermo-cleaved peptide in each solution was converted to a percentage of activity compared to the control solution (200 mM ammonium acetate). * $P < 0.005$ and ** $P < 0.05$. Error bars are shown as ± standard deviation ($n = 3$).

https://dx.doi.org/10.1021/acs.biochem.0c00105
Biochemistry 2020, 59, 1013−1022

the FT_2 tag on TTR propensity for thermo-decomposition in solution.

Relation between Metalloprotease Activity of TTR and Thermo-Cleavage. TTR is a known metalloprotease for which the preferential site for substrate cleavage has been determined as Lys > Ala > Arg > Leu ≥ Met > Phe.[67] A similarity between this trend and lysine cleavage observed in our studies prompted us to investigate the correlation between metallopeptidase activity of FT_2-TTR. The protease activity of untagged TTR is inhibited when metal is removed from solution using EDTA or *ortho*-phenantroline.[11] To test whether thermo-cleavage is related to peptidase activity of TTR, FT_2-TTR was incubated at 50 °C in the presence of DTPA (1 mM), a more potent metal chelator, and the degradation was decreased but was not completely inhibited compared to the control sample (TTR in 200 mM AA) (see Figure 5). The addition of divalent metals, i.e., Zn(II), Co(II), and Fe(II), can restore protease activity.[11] For example, the addition of an equimolar concentration of zinc produced more thermo-cleaved peptides (~1.7-fold), but excess zinc (1:280 molar ratio) decreased the cleavage product in agreement with previous results that excess zinc exhibits inhibitory effects.[11] This inhibition can be attributed to structural changes of TTR upon zinc binding to other sites, i.e., EF loop and increased backbone flexibility.[12] Unlike zinc, a low concentration of Cu(II) has shown an inhibitory effect on TTR proteolytic activity;[11] however, incubation of FT_2-TTR with an equimolar concentration of Cu(II) increased the amount of cleavage product (Figure 5).

DISCUSSION

Schneider et al.[41] reported similar thermodynamic stability of WT and FT_2-TTR using GdmHCl unfolding experiments. More recently, FT_2-TTR was shown to be more prone to aggregation (5−10%) and slightly less thermodynamically stable than WT-TTR.[68] The CIU and VT-ESI studies reveal increased gas- and solution-phase stabilities for FT_2-TTR at room temperature (Figure 1 and Figure 2); conversely, CD spectroscopy and VT-ESI suggest a decreased thermostability that might explain previously reported aggregation propensities of FT_2-TTR.[68] A recent study by El-Baba et al.[56] illustrates increased sensitivity of native IM-MS compared to other methods; they used VT-ESI combined with native MS and IM-MS and discovered several new intermediates in the unfolding pathway of ubiquitin. Here, we used a similar approach in an effort to better assess the effects of tags on the TTR structure.

Collectively, the experimental results suggest that the mechanism of increased stability of FT_2-TTR, compared to WT- and CT-TTR at room temperature (Figure 2), can be attributed to interactions between the FT_2 tag and N-terminal domain of TTR, which is favorable due to their close proximity. Charged residues of the N-terminus, e.g., E and K, can readily form salt bridges with the FT_2 tag by hydrogen bond interactions involving the lysine and aspartic acid residues. The increased gas-phase stability of FT_2-TTR compared to WT- and CT-TTR in CIU experiments (Figure 1) is consistent with previous studies where electrostatic interactions are enhanced and are dominant for desolvated ions in the gas phase.[69]

Similar to other proteins, the N-terminal domain of TTR is very dynamic, and only a single crystal structure is atomically resolved containing this domain (PDB 1ttc).[70] Despite such flexibility, this domain has a huge impact on TTR structure, and several hydrogen bonds have been assigned between residues Thr59 and Thr60 and N-terminal residues, i.e., Gly4, Gly6, and Ser8 (Figure S12). Previous studies also point to involvement of the N-terminus in metal binding,[12] ligand binding,[4,71] and amyloidosis. Specifically, Cys10 is involved in the first zinc binding site,[12] and its modifications, i.e., oxidation, sulfonation, and cysteinylation, have been shown to alter amyloidogenesis of wild-type TTR and mutants.[14,72−74] FT_2 tag interaction with the N-terminal domain of TTR can decrease the flexibility of this domain and thus increase the TTR stability.

Despite increased stability at room temperature, the observed thermo-cleavage of only the N-terminus of FT_2-TTR indicates that amino acid residues in the tag destabilize the secondary structure of TTR at elevated temperatures. This result was further confirmed with CD spectroscopy as some batches showed slightly lower thermostability (Figure S8). A comprehensive study on proteome scale analysis of thermostability of different cells has shown higher relative abundance of aspartic acid residues in thermally unstable proteins.[75] Our data corroborate the destabilization effect of multiple aspartic acid residues on the FT_2 tag, which decreases FT_2-TTR thermal stability in solution. Our data suggest that the N-terminal domain of TTR is not a suitable region for structural modification. Also, tag-induced structural change and the infusion domain, N-terminus vs C-terminus, are needed to be studied case by case for any protein of interest.

Previously, Gouvea et al.[76] have studied the metalloprotease activity of TTR and demonstrated that a single basic residue, probably lysine, and one acidic residue are involved in the proteolysis site of TTR. Liz et al.[11] also identified the active site of TTR using the site-directed mutagenesis approach, where Glu89 plays a key role in stabilizing His88 in Zn coordination. Thus, several lysine and aspartic acid residues in the sequence of the FT_2 tag can influence and/or create a new binding site for the metalloprotease activity of TTR.

The fact that FT_2-TTR is detected intact after incubation for several days at high temperatures suggests that only a fraction of protein has peptidase activity. Previous studies have shown that only ~7% of TTR is enzymatically active,[11] which can be due to several metal binding sites, i.e., three for zinc binding,[12] as well as conformational heterogeneity of TTR revealed via NMR studies.[77] While mechanistic details of the thermo-cleavage of FT_2-TTR are not resolved, inhibition of thermo-cleavage by DTPA and excess zinc points to correlation with the proteolysis activity of TTR. However, complete inhibition was not achieved in any solution tested in this study, which implies that other pathways are involved in the observed thermo-cleavage. Controversial results, in terms of observed increases in protease activity of FT_2-TTR in the presence of copper and reported inhibitory role of copper in TTR metalloprotease activity,[11] are likely due to the higher affinity of the FT_2 tag toward copper (Figure S10). Copper sequestration by the tag can diminish the inhibitory effect of copper, which we attribute to the substitution of zinc in the active site. Reduction of endogenous copper(II) to (I) by TCEP can justify more degradation of FT_2-TTR with TCEP addition, which diminishes the inhibitory effect of copper.[78]

CONCLUSION

Purification tags have undoubtedly facilitated the purification of recombinant proteins; however, they can alter the dynamics and function of proteins. The results presented here clearly

https://dx.doi.org/10.1021/acs.biochem.0c00105
Biochemistry 2020, 59, 1013−1022

illustrate the stabilizing effects of the dual-FLAG tag on the quaternary structure of TTR at room temperature, whereas, at elevated temperatures, metal ions (Zn and Cu) present in the solution are directly linked to a backbone cleavage reaction between Lys9 and Cys10. While metal removal or excess zinc inhibited cleavage similar to the previously reported metalloprotease activity of TTR, equimolar zinc or copper increased the thermal cleavage. The mechanism of metal-induced cleavage was revealed by combinations of variable-temperature native MS and IM-MS. This study shows that the N-terminal domain of TTR is not suitable for affinity tag insertion. This study further illustrates the utility of native IM-MS for detailed structural analyses of proteins.

■ ASSOCIATED CONTENT

Supporting Information

The Supporting Information is available free of charge at https://pubs.acs.org/doi/10.1021/acs.biochem.0c00105.

Description of mass and charge dependency calculations, tuning parameters for mass spectrometry, schematic of the VT-ESI source, secondary structure analysis and melting experiments using CD spectroscopy, CIU plots of charge reduced WT-, CT-, and FT_2-TTR, mass spectrum of gas-phase activation of thermally heated FT_2-TTR, and mass spectrum of the isolated thermocleaved peptide without and with copper and zinc (PDF)

Accession Codes

TTR: P02766.

■ AUTHOR INFORMATION

Corresponding Author

David H. Russell − *Department of Chemistry, Texas A & M University, College Station, Texas 77843, United States;* orcid.org/0000-0003-0830-3914; Email: russell@chem.tamu.edu

Authors

Mehdi Shirzadeh − *Department of Chemistry, Texas A & M University, College Station, Texas 77843, United States*

Michael L. Poltash − *Department of Chemistry, Texas A & M University, College Station, Texas 77843, United States*

Arthur Laganowsky − *Department of Chemistry, Texas A & M University, College Station, Texas 77843, United States;* orcid.org/0000-0001-5012-5547

Complete contact information is available at: https://pubs.acs.org/10.1021/acs.biochem.0c00105

Funding

This work is supported by funds from the National Science Foundation (CHE1707675) and the National Institutes of Health (RO1 GM121751 and P41GM128577).

Notes

The authors declare no competing financial interest.

■ ACKNOWLEDGMENTS

We thank Dr. Gloria M. Conover for the construction of the FT_2-TTR plasmid. We would like to thank Shelby Oney for assistance in collecting the CD data. We also appreciate reviewers for their constructive comments.

■ REFERENCES

(1) Hornberg, A., Eneqvist, T., Olofsson, A., Lundgren, E., and Sauer-Eriksson, A. E. (2000) A comparative analysis of 23 structures of the amyloidogenic protein transthyretin. *J. Mol. Biol. 302*, 649−669.

(2) Hennebry, S. C. (2009) Evolutionary changes to transthyretin: structure and function of a transthyretin-like ancestral protein. *FEBS J. 276*, 5367−5379.

(3) Schreiber, G., and Richardson, S. J. (1997) The Evolution of Gene Expression, Structure and Function of Transthyretin. *Comp. Biochem. Physiol., Part B: Biochem. Mol. Biol. 116*, 137−160.

(4) Chang, L., Munro, S. L., Richardson, S. J., and Schreiber, G. (1999) Evolution of thyroid hormone binding by transthyretins in birds and mammals. *Eur. J. Biochem. 259*, 534−542.

(5) Monaco, H. L., Rizzi, M., and Coda, A. (1995) Structure of a complex of two plasma proteins: transthyretin and retinol-binding protein. *Science 268*, 1039−1041.

(6) Fleming, C. E., Mar, F. M., Franquinho, F., and Sousa, M. M. (2009) Chapter 17 Transthyretin: An Enhancer of Nerve Regeneration, In *International Review of Neurobiology*, pp 337−346, Academic Press.

(7) Reixach, N., Deechongkit, S., Jiang, X., Kelly, J. W., and Buxbaum, J. N. (2004) Tissue damage in the amyloidoses: Transthyretin monomers and nonnative oligomers are the major cytotoxic species in tissue culture. *Proc. Natl. Acad. Sci. U. S. A. 101*, 2817−2822.

(8) Ueda, M., and Ando, Y. (2014) Recent advances in transthyretin amyloidosis therapy. *Transl. Neurodegener. 3*, 19.

(9) Adams, D., Koike, H., Slama, M., and Coelho, T. (2019) Hereditary transthyretin amyloidosis: a model of medical progress for a fatal disease. *Nat. Rev. Neurol. 15*, 387−404.

(10) Understanding and Ameliorating the TTR Amyloidoses, In *Protein Misfolding Diseases*, pp 967−1003.

(11) Liz, M. A., Leite, S. C., Juliano, L., Saraiva, M. J., Damas, A. M., Bur, D., and Sousa, M. M. (2012) Transthyretin is a metallopeptidase with an inducible active site. *Biochem. J. 443*, 769−778.

(12) Palmieri, L. d. C., Lima, L. M. T. R., Freire, J. B. B., Bleicher, L., Polikarpov, I., Almeida, F. C. L., and Foguel, D. (2010) Novel Zn2+-binding sites in human transthyretin: implications for amyloidogenesis and retinol-binding protein recognition. *J. Biol. Chem. 285*, 31731−31741.

(13) Wilkinson-White, L. E., and Easterbrook-Smith, S. B. (2007) Characterization of the binding of Cu(II) and Zn(II) to transthyretin: effects on amyloid formation. *Biochemistry 46*, 9123−9132.

(14) Poltash, M. L., Shirzadeh, M., McCabe, J. W., Moghadamchargari, Z., Laganowsky, A., and Russell, D. H. (2019) New insights into the metal-induced oxidative degradation pathways of transthyretin. *Chem. Commun. (Cambridge, U. K.) 55*, 4091−4094.

(15) Arnau, J., Lauritzen, C., Petersen, G. E., and Pedersen, J. (2006) Current strategies for the use of affinity tags and tag removal for the purification of recombinant proteins. *Protein Expression Purif. 48*, 1−13.

(16) Vandemoortele, G., Eyckerman, S., and Gevaert, K. (2019) Pick a Tag and Explore the Functions of Your Pet Protein. *Trends Biotechnol. 37*, 1078−1090.

(17) Carson, M., Johnson, D. H., McDonald, H., Brouillette, C., and Delucas, L. J. (2007) His-tag impact on structure. *Acta Crystallogr., Sect. D: Biol. Crystallogr. 63*, 295−301.

(18) Booth, W. T., Schlachter, C. R., Pote, S., Ussin, N., Mank, N. J., Klapper, V., Offermann, L. R., Tang, C., Hurlburt, B. K., and Chruszcz, M. (2018) Impact of an N-terminal Polyhistidine Tag on Protein Thermal Stability. *ACS Omega 3*, 760−768.

(19) Yewdall, N. A., Allison, T. M., Pearce, F. G., Robinson, C. V., and Gerrard, J. A. (2018) Self-assembly of toroidal proteins explored using native mass spectrometry. *Chem. Sci. 9*, 6099−6106.

(20) Geoghegan, K. F., Dixon, H. B., Rosner, P. J., Hoth, L. R., Lanzetti, A. J., Borzilleri, K. A., Marr, E. S., Pezzullo, L. H., Martin, L. B., LeMotte, P. K., McColl, A. S., Kamath, A. V., and Stroh, J. G. (1999) Spontaneous alpha-N-6-phosphogluconoylation of a "His tag"

in Escherichia coli: the cause of extra mass of 258 or 178 Da in fusion proteins. *Anal. Biochem. 267*, 169−184.
(21) Liu, Y., LoCaste, C. E., Liu, W., Poltash, M. L., Russell, D. H., and Laganowsky, A. (2019) Selective binding of a toxin and phosphatidylinositides to a mammalian potassium channel. *Nat. Commun. 10*, 1352.
(22) Kapust, R. B., and Waugh, D. S. (1999) Escherichia coli maltose-binding protein is uncommonly effective at promoting the solubility of polypeptides to which it is fused. *Protein Sci. 8*, 1668−1674.
(23) Waugh, D. S. (2005) Making the most of affinity tags. *Trends Biotechnol. 23*, 316−320.
(24) Taylor, E. J., Goyal, A., Guerreiro, C. I., Prates, J. A., Money, V. A., Ferry, N., Morland, C., Planas, A., Macdonald, J. A., Stick, R. V., Gilbert, H. J., Fontes, C. M., and Davies, G. J. (2005) How family 26 glycoside hydrolases orchestrate catalysis on different polysaccharides: structure and activity of a Clostridium thermocellum lichenase, CtLic26A. *J. Biol. Chem. 280*, 32761−32767.
(25) Chant, A., Kraemer-Pecore, C. M., Watkin, R., and Kneale, G. G. (2005) Attachment of a histidine tag to the minimal zinc finger protein of the Aspergillus nidulans gene regulatory protein AreA causes a conformational change at the DNA-binding site. *Protein Expression Purif. 39*, 152−159.
(26) Johnson, C. M. (2013) Differential scanning calorimetry as a tool for protein folding and stability. *Arch. Biochem. Biophys. 531*, 100−109.
(27) Greenfield, N. J. (2006) Using circular dichroism collected as a function of temperature to determine the thermodynamics of protein unfolding and binding interactions. *Nat. Protoc. 1*, 2527−2535.
(28) Huynh, K., and Partch, C. L. (2015) Analysis of protein stability and ligand interactions by thermal shift assay. *Curr. Protoc Protein Sci. 79*, 282921−282914.
(29) Pantoliano, M. W., Petrella, E. C., Kwasnoski, J. D., Lobanov, V. S., Myslik, J., Graf, E., Carver, T., Asel, E., Springer, B. A., Lane, P., and Salemme, F. R. (2001) High-density miniaturized thermal shift assays as a general strategy for drug discovery. *J. Biomol. Screening 6*, 429−440.
(30) Leney, A. C., and Heck, A. J. (2017) Native Mass Spectrometry: What is in the Name? *J. Am. Soc. Mass Spectrom. 28*, 5−13.
(31) Mehmood, S., Allison, T. M., and Robinson, C. V. (2015) Mass spectrometry of protein complexes: from origins to applications. *Annu. Rev. Phys. Chem. 66*, 453−474.
(32) Hernandez, H., and Robinson, C. V. (2007) Determining the stoichiometry and interactions of macromolecular assemblies from mass spectrometry. *Nat. Protoc. 2*, 715−726.
(33) Snijder, J., Rose, R. J., Veesler, D., Johnson, J. E., and Heck, A. J. (2013) Studying 18 MDa virus assemblies with native mass spectrometry. *Angew. Chem., Int. Ed. 52*, 4020−4023.
(34) Sharon, M., and Robinson, C. V. (2007) The role of mass spectrometry in structure elucidation of dynamic protein complexes. *Annu. Rev. Biochem. 76*, 167−193.
(35) Cong, X., Liu, Y., Liu, W., Liang, X., Russell, D. H., and Laganowsky, A. (2016) Determining Membrane Protein-Lipid Binding Thermodynamics Using Native Mass Spectrometry. *J. Am. Chem. Soc. 138*, 4346−4349.
(36) Ruotolo, B. T., Hyung, S. J., Robinson, P. M., Giles, K., Bateman, R. H., and Robinson, C. V. (2007) Ion mobility-mass spectrometry reveals long-lived, unfolded intermediates in the dissociation of protein complexes. *Angew. Chem., Int. Ed. 46*, 8001−8004.
(37) Hyung, S. J., Robinson, C. V., and Ruotolo, B. T. (2009) Gas-phase unfolding and disassembly reveals stability differences in ligand-bound multiprotein complexes. *Chem. Biol. 16*, 382−390.
(38) Hopper, J. T., and Oldham, N. J. (2009) Collision induced unfolding of protein ions in the gas phase studied by ion mobility-mass spectrometry: the effect of ligand binding on conformational stability. *J. Am. Soc. Mass Spectrom. 20*, 1851−1858.
(39) Saelices, L., Johnson, L. M., Liang, W. Y., Sawaya, M. R., Cascio, D., Ruchala, P., Whitelegge, J., Jiang, L., Riek, R., and Eisenberg, D. S. (2015) Uncovering the Mechanism of Aggregation of Human Transthyretin. *J. Biol. Chem. 290*, 28932−28943.
(40) Hammarstrom, P., Schneider, F., and Kelly, J. W. (2001) Trans-suppression of misfolding in an amyloid disease. *Science 293*, 2459−2462.
(41) Schneider, F., Hammarstrom, P., and Kelly, J. W. (2001) Transthyretin slowly exchanges subunits under physiological conditions: A convenient chromatographic method to study subunit exchange in oligomeric proteins. *Protein Sci. 10*, 1606−1613.
(42) Shirzadeh, M., Boone, C. D., Laganowsky, A., and Russell, D. H. (2019) Topological Analysis of Transthyretin Disassembly Mechanism: Surface-Induced Dissociation Reveals Hidden Reaction Pathways. *Anal. Chem. 91*, 2345−2351.
(43) Rappley, I., Monteiro, C., Novais, M., Baranczak, A., Solis, G., Wiseman, R. L., Helmke, S., Maurer, M. S., Coelho, T., Powers, E. T., and Kelly, J. W. (2014) Quantification of transthyretin kinetic stability in human plasma using subunit exchange. *Biochemistry 53*, 1993−2006.
(44) Polasky, D. A., Dixit, S. M., Fantin, S. M., and Ruotolo, B. T. (2019) CIUSuite 2: Next-Generation Software for the Analysis of Gas-Phase Protein Unfolding Data. *Anal. Chem. 91*, 3147−3155.
(45) Ruotolo, B. T., Benesch, J. L., Sandercock, A. M., Hyung, S. J., and Robinson, C. V. (2008) Ion mobility-mass spectrometry analysis of large protein complexes. *Nat. Protoc. 3*, 1139−1152.
(46) Bush, M. F., Hall, Z., Giles, K., Hoyes, J., Robinson, C. V., and Ruotolo, B. T. (2010) Collision cross sections of proteins and their complexes: a calibration framework and database for gas-phase structural biology. *Anal. Chem. 82*, 9557−9565.
(47) Sterling, H. J., Cassou, C. A., Susa, A. C., and Williams, E. R. (2012) Electrothermal supercharging of proteins in native electrospray ionization. *Anal. Chem. 84*, 3795−3801.
(48) Pan, J., Xu, K., Yang, X., Choy, W. Y., and Konermann, L. (2009) Solution-phase chelators for suppressing nonspecific protein-metal interactions in electrospray mass spectrometry. *Anal. Chem. 81*, 5008−5015.
(49) Dixit, S. M., Polasky, D. A., and Ruotolo, B. T. (2018) Collision induced unfolding of isolated proteins in the gas phase: past, present, and future. *Curr. Opin. Chem. Biol. 42*, 93−100.
(50) Dixit, S. M., Polasky, D. A., and Ruotolo, B. T. (2018) Collision induced unfolding of isolated proteins in the gas phase: past, present, and future. *Curr. Opin. Chem. Biol. 42*, 93−100.
(51) Han, L., Hyung, S. J., Mayers, J. J., and Ruotolo, B. T. (2011) Bound anions differentially stabilize multiprotein complexes in the absence of bulk solvent. *J. Am. Chem. Soc. 133*, 11358−11367.
(52) Han, L., Hyung, S. J., and Ruotolo, B. T. (2012) Bound cations significantly stabilize the structure of multiprotein complexes in the gas phase. *Angew. Chem., Int. Ed. 51*, 5692−5695.
(53) Dong, S., Wagner, N. D., and Russell, D. H. (2018) Collision-Induced Unfolding of Partially Metalated Metallothionein-2A: Tracking Unfolding Reactions of Gas-Phase Ions. *Anal. Chem. 90*, 11856−11862.
(54) Eschweiler, J. D., Martini, R. M., and Ruotolo, B. T. (2017) Chemical Probes and Engineered Constructs Reveal a Detailed Unfolding Mechanism for a Solvent-Free Multidomain Protein. *J. Am. Chem. Soc. 139*, 534−540.
(55) Zhong, Y., Han, L., and Ruotolo, B. T. (2014) Collisional and Coulombic unfolding of gas-phase proteins: high correlation to their domain structures in solution. *Angew. Chem., Int. Ed. 53*, 9209−9212.
(56) El-Baba, T. J., Woodall, D. W., Raab, S. A., Fuller, D. R., Laganowsky, A., Russell, D. H., and Clemmer, D. E. (2017) Melting Proteins: Evidence for Multiple Stable Structures upon Thermal Denaturation of Native Ubiquitin from Ion Mobility Spectrometry-Mass Spectrometry Measurements. *J. Am. Chem. Soc. 139*, 6306−6309.
(57) Kohler, M., Marchand, A., Hentzen, N. B., Egli, J., Begley, A. I., Wennemers, H., and Zenobi, R. (2019) Temperature-controlled

https://dx.doi.org/10.1021/acs.biochem.0c00105
Biochemistry 2020, 59, 1013−1022

electrospray ionization mass spectrometry as a tool to study collagen homo- and heterotrimers. *Chem. Sci. 10*, 9829−9835.
(58) Wang, G., Bondarenko, P. V., and Kaltashov, I. A. (2018) Multi-step conformational transitions in heat-treated protein therapeutics can be monitored in real time with temperature-controlled electrospray ionization mass spectrometry. *Analyst 143*, 670−677.
(59) El-Baba, T. J., Fuller, D. R., Woodall, D. W., Raab, S. A., Conant, C. R., Dilger, J. M., Toker, Y., Williams, E. R., Russell, D. H., and Clemmer, D. E. (2018) Melting proteins confined in nanodroplets with 10.6 mum light provides clues about early steps of denaturation. *Chem. Commun. (Cambridge, U. K.) 54*, 3270−3273.
(60) Shnyrov, V. L., Villar, E., Zhadan, G. G., Sanchez-Ruiz, J. M., Quintas, A., Saraiva, M. J., and Brito, R. M. (2000) Comparative calorimetric study of non-amyloidogenic and amyloidogenic variants of the homotetrameric protein transthyretin. *Biophys. Chem. 88*, 61−67.
(61) Breuker, K., and McLafferty, F. W. (2008) Stepwise evolution of protein native structure with electrospray into the gas phase, 10(−12) to 10(2) s. *Proc. Natl. Acad. Sci. U. S. A. 105*, 18145−18152.
(62) Silveira, J. A., Fort, K. L., Kim, D., Servage, K. A., Pierson, N. A., Clemmer, D. E., and Russell, D. H. (2013) From solution to the gas phase: stepwise dehydration and kinetic trapping of substance P reveals the origin of peptide conformations. *J. Am. Chem. Soc. 135*, 19147−19153.
(63) Jurchen, J. C., Cooper, R. E., and Williams, E. R. (2003) The role of acidic residues and of sodium ion adduction on the gas-phase H/D exchange of peptides and peptide dimers. *J. Am. Soc. Mass Spectrom. 14*, 1477−1487.
(64) Verkerk, U. H., and Kebarle, P. (2005) Ion-ion and ion−molecule reactions at the surface of proteins produced by nanospray. Information on the number of acidic residues and control of the number of ionized acidic and basic residues. *J. Am. Soc. Mass Spectrom. 16*, 1325−1341.
(65) Zhang, S., and Basile, F. (2007) Site-specific pyrolysis-induced cleavage at aspartic acid residue in peptides and proteins. *J. Proteome Res. 6*, 1700−1704.
(66) Basile, F., Zhang, S., Kandar, S. K., and Lu, L. (2011) Mass spectrometry characterization of the thermal decomposition/digestion (TDD) at cysteine in peptides and proteins in the condensed phase. *J. Am. Soc. Mass Spectrom. 22*, 1926−1940.
(67) Liz, M. A., Fleming, C. E., Nunes, A. F., Almeida, M. R., Mar, F. M., Choe, Y., Craik, C. S., Powers, J. C., Bogyo, M., and Sousa, M. M. (2009) Substrate specificity of transthyretin: identification of natural substrates in the nervous system. *Biochem. J. 419*, 467−474.
(68) Robinson, L. Z., and Reixach, N. (2014) Quantification of quaternary structure stability in aggregation-prone proteins under physiological conditions: the transthyretin case. *Biochemistry 53*, 6496−6510.
(69) Breuker, K., Bruschweiler, S., and Tollinger, M. (2011) Electrostatic stabilization of a native protein structure in the gas phase. *Angew. Chem., Int. Ed. 50*, 873−877.
(70) Hamilton, J. A., Steinrauf, L. K., Braden, B. C., Liepnieks, J., Benson, M. D., Holmgren, G., Sandgren, O., and Steen, L. (1993) The x-ray crystal structure refinements of normal human transthyretin and the amyloidogenic Val-30–>Met variant to 1.7-A resolution. *J. Biol. Chem. 268*, 2416−2424.
(71) Prapunpoj, P., Leelawatwatana, L., Schreiber, G., and Richardson, S. J. (2006) Change in structure of the N-terminal region of transthyretin produces change in affinity of transthyretin to T4 and T3. *FEBS J. 273*, 4013−4023.
(72) Kingsbury, J. S., Laue, T. M., Klimtchuk, E. S., Theberge, R., Costello, C. E., and Connors, L. H. (2008) The modulation of transthyretin tetramer stability by cysteine 10 adducts and the drug diflunisal. Direct analysis by fluorescence-detected analytical ultracentrifugation. *J. Biol. Chem. 283*, 11887−11896.
(73) Takaoka, Y., Ohta, M., Miyakawa, K., Nakamura, O., Suzuki, M., Takahashi, K., Yamamura, K.-i., and Sakaki, Y. (2004) Cysteine 10 Is a Key Residue in Amyloidogenesis of Human Transthyretin Val30Met. *Am. J. Pathol. 164*, 337−345.
(74) Zhang, Q., and Kelly, J. W. (2003) Cys10 mixed disulfides make transthyretin more amyloidogenic under mildly acidic conditions. *Biochemistry 42*, 8756−8761.
(75) Leuenberger, P., Ganscha, S., Kahraman, A., Cappelletti, V., Boersema, P. J., von Mering, C., Claassen, M., and Picotti, P. (2017) Cell-wide analysis of protein thermal unfolding reveals determinants of thermostability. *Science 355*, No. eaai7825.
(76) Gouvea, I. E., Kondo, M. Y., Assis, D. M., Alves, F. M., Liz, M. A., Juliano, M. A., and Juliano, L. (2013) Studies on the peptidase activity of transthyretin (TTR). *Biochimie 95*, 215−223.
(77) Sun, X., Dyson, H. J., and Wright, P. E. (2018) Kinetic analysis of the multistep aggregation pathway of human transthyretin. *Proc. Natl. Acad. Sci. U. S. A. 115*, E6201−E6208.
(78) Krezel, A., Latajka, R., Bujacz, G. D., and Bal, W. (2003) Coordination properties of tris(2-carboxyethyl)phosphine, a newly introduced thiol reductant, and its oxide. *Inorg. Chem. 42*, 1994−2003.

https://dx.doi.org/10.1021/acs.biochem.0c00105
Biochemistry 2020, 59, 1013−1022